Stability and dynamics of carbon and nitrogen dopants in anatase TiO_2: A density functional theory study

L. Tsetseris
Department of Physics, National Technical University of Athens, GR-15780 Athens, Greece;
Department of Physics, Aristotle University of Thessaloniki, GR-54124 Thessaloniki, Greece;
and Department of Physics and Astronomy, Vanderbilt University, Nashville, Tennessee 37235, USA
(Received 28 September 2009; revised manuscript received 30 March 2010; published 22 April 2010)

The properties of carbon- and nitrogen-doped anatase TiO_2, a renowned photocatalyst, depend strongly on the atomic-scale details of dopant incorporation and dynamics. Here we identify with *ab initio* calculations stable structures of C dopants in TiO_2 that differ from previous theoretical predictions. We also describe the evolution of dopants and point defects in terms of diffusion barriers and defect complex formation. In particular, we study processes that allow dopants and oxygen native defects to migrate and initiate dopant transformations. The results reveal a range of growth and annealing conditions that can create, shift, or annihilate levels in the TiO_2 band gap, altering significantly its catalytic activity.

DOI: 10.1103/PhysRevB.81.165205 PACS number(s): 66.30.J−, 61.72.up

I. INTRODUCTION

The photodissociation of important chemical compounds such as water[1] or pollutants[2,3] on titania surfaces and the promising role of TiO_2 in photovoltaic applications[4,5] have spurred intense research efforts to optimize the catalytic and energy-conversion properties of TiO_2-based systems. A significant portion of these efforts[2,5–21] relates to doping of TiO_2 with metal and nonmetal atoms. The large energy band gap, more than 3.0 eV, of the most prevalent TiO_2 crystal structures (rutile and anatase) limits the TiO_2 efficiency for visible light absorption and, concomitantly, the photocatalytic performance. Doping, in general, is accepted as a means to enhance absorption by either narrowing the TiO_2 energy gap or by creating levels in the gap. Nevertheless, which of these two mechanisms prevails in a particular doping scheme is often the subject of debate.

Nitrogen and carbon are the most widely used species for nonmetal doping of TiO_2. Experiments[6,7] have shown N- and C-doped TiO_2 to be better visible light absorbers than pristine titania, and theoretical studies have provided a wealth of information that links the presence of C and N dopants to reduced TiO_2 band gap[6,17,18,21] or levels in the gap.[11,12,16,19,20] Naturally, the impact of impurities on the electronic properties of the host system is determined by their concentration and the structural details of their most stable configurations. Another important factor is the interaction between impurities and native defects. For example, theoretical studies have found[12,15] that the formation energy of oxygen vacancies in TiO_2 is reduced in the presence of N dopants. For these reasons, the stability of impurities and pertinent dynamical effects such as diffusion of dopants and defects are key factors for the variation in the catalytic efficiency of TiO_2 samples with respect to growth or annealing processes.

In this paper, we report the results of extensive first-principles calculations on the stability of C and N dopant configurations in anatase TiO_2, the diffusion barriers of dopants and point defects, as well as their mutual interactions. We find that the most stable C configurations are different than those reported in previous studies, at least for low concentrations of dopants, and we describe the impact of transformations between substitutional and interstitial dopant configurations on the electronic properties of doped TiO_2. The conditions that favor such transformations are addressed in terms of diffusion barriers and interaction energies of dopants and TiO_2 point defects. Specifically, for the latter we probe their diffusivity and their tendency to form complexes with dopants. Overall, the results address several processes that can modify the catalytic activity of TiO_2 through annealing and changes in stoichiometry.

II. METHOD

The results were obtained with the density functional theory (DFT) code VASP.[22] We employed projector-augmented wave potentials[23] and a generalized-gradient approximation (GGA) corrected exchange-correlation functional.[24] The cutoff for the plane-wave basis was set at 400 eV. Unless stated otherwise, the calculations were performed with the anatase lattice constants fixed at the experimental values[25] and employed $3\times3\times1$ supercells with 36 Ti and 72 O atoms in the pristine TiO_2 case. The total-energy differences reported below are based on converged k-space sampling[26] with $3\times3\times3$ k grids. The electronic density of states (DOS) calculations employed the tetrahedron method[27] and a finer $7\times7\times7$ k grid.

The so-called minimum-energy pathways (MEPs) for transformations between dopant configurations are obtained with the nudged elastic band (NEB) method.[28] The transition states correspond to the saddle points along these pathways. The energy difference between the highest transition state and the most stable dopant configuration provides the activation energy of a process. A MEP is simulated within the NEB method as a sequence of intermediate configurations which are termed as images. Each sequence comprises 16 images between nearest local-energy minimum configurations. The choice of number of images and convergence criteria for the NEB calculations is based on agreement between measured activation energies and pertinent results in similar computational studies on Ti-based[29,30] materials and other[31,32] sys-

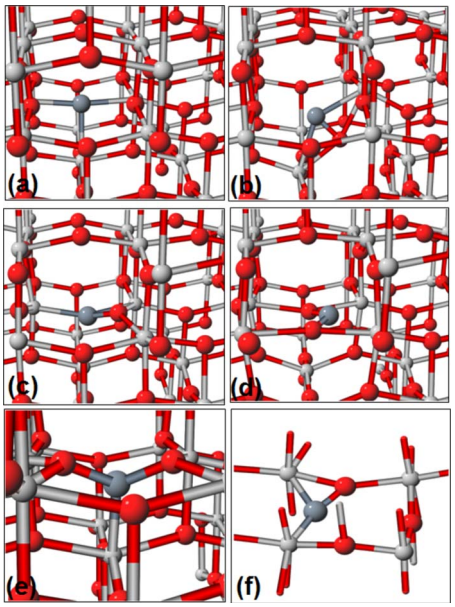

FIG. 1. (Color online) Configurations of substitutional C dopants (shown with arrows) in anatase TiO_2. Compared to the most stable structure (c), the energies of (a), (b), (d), and (e) are 1.21 eV, 0.53 eV, 0.61 eV, and 0.41 eV higher, respectively. The diffusion barrier is 1.77 eV. (f) is a zoomed-in depiction of (c). [Ti: light gray, O: dark gray (red), and C: gray spheres.]

tems. To obtain migration activation energies, one must study transformations between the lowest-energy structures. In principle, these transformations may go through other intermediate metastable structures. As we will see below, this multistep feature is indeed present in transformations of dopants in anatase TiO_2. In some cases, relaxation of one MEP with the NEB method gives rise to a new local energy minimum. The MEP is then dissected to two consecutive processes.[33] In fact, this is the way how a number of the lowest-energy carbon dopant structures were obtained. All the NEB calculations were performed using Γ-point sampling of k space, with the exception of the MEP segments that include the rate-limiting step of each process. For these segments, the calculations were refined with sampling based on $2\times2\times2$ and $3\times3\times3$ k grids to ensure convergence for the reported activation energies.

III. RESULTS

A. Carbon-doped TiO_2

Intuitively, substitutional dopants could be expected to occupy the crystal sites of the atoms they replace. The corresponding structure (C_s^a) for C-doped TiO_2 is shown in Fig. 1(a) and it has been the subject of pertinent theoretical studies.[20,21] It has already been shown,[19] however, that C_s^a is, in fact, a metastable configuration, and that the structure (C_s^e) of Fig. 1(e) has a lower energy. Our results confirm that C_s^e lies about 0.8 eV lower than C_s^a but also find its energy to be 0.41 eV higher than that of the most stable configuration C_s^c of Fig. 1(c). One possible reason for this discrepancy might be the fact that these values correspond to a dopant concentration which is lower than that used in previous studies.[19] In the C_s^c structure, the C dopant is displaced away from the substitutional position and forms a bond to a nearest O atom. A detail of the structure is shown also in Fig. 1(f). In the C_s^e arrangement, the C dopant is also displaced with respect to the substitutional position but it forms bonds to two nearest O atoms, as well as to a Ti atom. The results on the energies and spin polarizations of the most stable dopant configurations are summarized in Table I.

TABLE I. Energies and magnetic moments (M) for the most stable configurations of substitutional C (C_s), interstitial C (C_i), substitutional N (N_s), and interstitial N (N_i) impurities in anatase TiO_2. For N_s, the mentioned structures resemble the C_s configurations of Fig. 1.

Impurity type	Configuration	Energy (eV)	M (μ_B)
C_s	Fig. 1(a)	1.21	0.00
C_s	Fig. 1(b)	0.53	0.00
C_s	Fig. 1(c)	0.00	0.00
C_s	Fig. 1(d)	0.61	0.00
C_s	Fig. 1(e)	0.41	0.00
C_i	Fig. 3(a)	0.00	0.00
C_i	Fig. 3(b)	0.31	0.00
C_i	Fig. 3(c)	0.73	0.00
C_i	Fig. 3(d)	0.31	0.00
N_s	Fig. 1(a)	0.00	1.00
N_s	Fig. 1(b)	1.53	0.00
N_s	Fig. 1(c)	0.90	0.00
N_s	Fig. 1(d)	3.60	0.00
N_i	Fig. 6	0.00	1.00

When the C dopant and its nearest O atom of C_s^c exchange their positions, a new configuration of the C_s^c type is obtained. The activation energy (E_a) for the exchange process is equal to 1.77 eV. The energy variation and intermediate configurations of this transformation are depicted in Fig. 2. The latter C_s^c structure can further transform to C_s^d with an energy barrier of 0.6 eV. On the other hand, the first C_s^c structure of Fig. 1(c) may transform to C_s^b. The process has a barrier of 0.8 eV and an energy penalty of 0.53 eV. The combination of the above steps allows for migration of substitutional C dopants with a diffusion barrier of 1.77 eV. Another migration path with a high E_a of 2.75 eV comprises transformation of C_s^c to C_s^b and a rate-limiting exchange of positions between the C dopant and its nearest O atom. Based on the calculated E_a's, we can conclude that the effective barrier for migration of substitutional C in TiO_2 is equal to 1.77 eV.

Similar to the case of substitutional C, interstitial C impurities in TiO_2 can attain several metastable configurations. Four such structures are shown in Fig. 3. In the most stable configuration (C_i^a) of Fig. 3(a), the C impurity binds to three O atoms in a planar geometry. A more detailed depiction of the defect is included in Fig. 3(e). The bond lengths between C and the three O atoms are equal to 1.31, 1.28, and 1.28 Å. To our knowledge, the identification of C_i^a as the lowest-

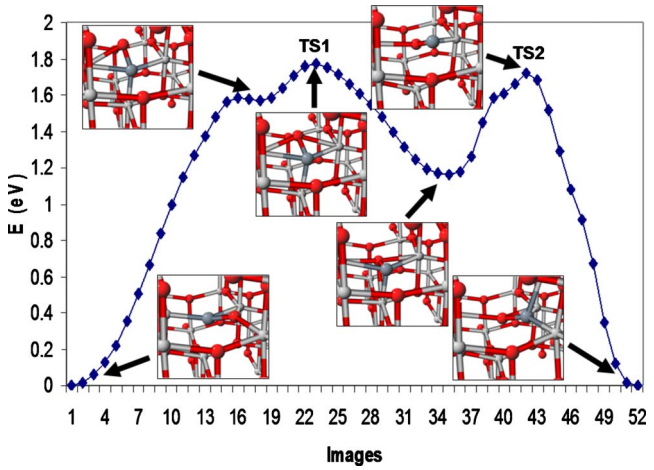

FIG. 2. (Color online) Energy variation and structures (insets) during exchange of positions for the C atom of Fig. 1(c) and its nearest O atom. TS1 and TS2 are the two transition states. [Ti: light gray, O: dark gray (red), and C: gray spheres.]

energy C interstitial structure is different than predictions of previous studies. For example, DFT studies[19] have identified as the most stable configuration the structure (C_i^b) depicted in Fig. 3(b), which is obtained when the C atom buckles out of the planar C_i^a structure. In particular, starting from C_i^a, the C_i^b structure is formed by moving the C dopant in the direction of the arrow in Fig. 3(a) so that it does not lie within the plane defined by its three nearest O atoms. Based on our results, however, the energy of C_i^b is 0.31 eV higher than that of C_i^a.

Various paths are possible for diffusion of C interstitials in TiO_2. In one path, C_i^a transforms to C_i^b and then to the C_i^c structure of Fig. 3(c). Subsequent transformations of C_i^c to neighboring C_i^b and, finally, to C_i^a structures can complete a migration step between lowest-energy C interstitial configurations. The barrier for this path is equal to 2.06 eV and the rate-limiting step is C_i^b to C_i^c transformation. Another path of lower E_a involves a multistep transformation of C_i^a to the C_i^d configuration of Fig. 3(d). The effective activation energy for this migration path is 1.86 eV and represents the diffusion barrier of C interstitials in anatase TiO_2.

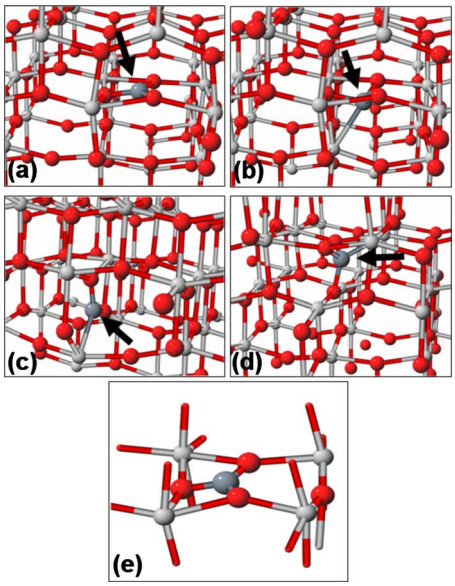

FIG. 3. (Color online) Configurations of interstitial C impurities (shown with arrows) in anatase TiO_2. The most stable structure is (a) while the energies of (b), (c), and (d) are 0.31 eV, 0.73 eV, and 0.31 eV higher, respectively. (e) is a detailed depiction of (a). The diffusion barrier is 1.86 eV and relates to transformations between (a) and (d). [Ti: light gray, O: dark gray (red), C: gray spheres.]

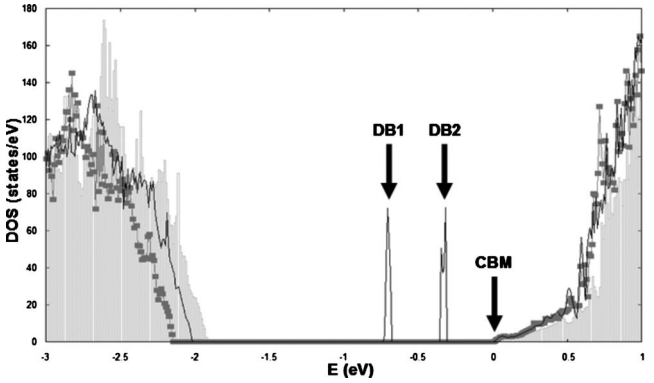

FIG. 4. Electronic DOS of pristine anatase TiO_2 (shaded) and TiO_2 with substitutional (solid line) and interstitial C (line with squares) impurities. Zero of energy is set at the conduction-band minimum (CBM). DB1 and DB2 denote the substitutional C-related defect gap states.

Figure 4 presents the electronic DOS of pristine anatase TiO_2 and TiO_2 with substitutional and interstitial C impurities in the most stable structures C_s^c and C_i^a we described above. The calculated band gap (1.91 eV) is comparable to the DFT value (2.0 eV) obtained by Asahi *et al.*[34] but much smaller than the experimental value (3.2 eV) due to well-known limitations of DFT. When C atoms are introduced as substitutional or interstitial impurities, the calculated band gap increases slightly to 2.0 eV and 2.1 eV, respectively. A significant difference between these two cases is the fact that while substitutional C creates defect levels (called DB1 and DB2 in Fig. 4) in the anatase band gap, interstitial C impurities do not create any such gap states. With respect to experiments, the existence of C-related gap states away from the valence- and conduction-band edges is consistent with the reported[7,8] visible light absorption by C-doped TiO_2. On the other hand, experiments[7,8] often find a redshift in the absorption by TiO_2 after C doping while a recent study[9] obtained a blueshift for C-doped rutile TiO_2. The results of Fig. 4 show an increase in the gap with the introduction of C impurities. Future studies will explore the effect of C impurities on the electronic properties of rutile TiO_2 and whether C dopants in complexes with other impurities or defects may lead to gap narrowing.

B. Nitrogen-doped TiO_2

The configurations of Fig. 1 are, allowing for small differences in bond lengths and overall relaxation, local equilibrium structures also for substitutional N dopants in anatase TiO_2. In analogy to the C case, let us call these structures N_s^a,

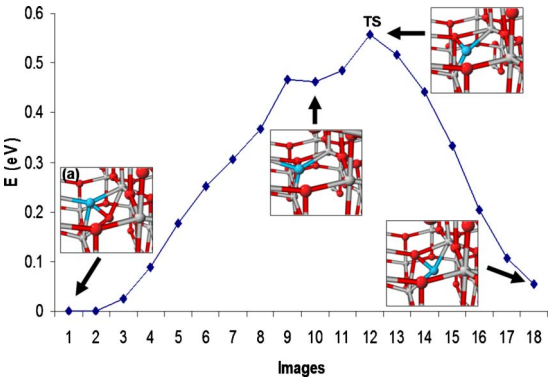

FIG. 5. (Color online) Energy variation and structures (insets) during exchange of positions for a substitutional N atom and its nearest O atom in TiO_2. TS is the transition state. The reference energy for this figure [the energy of inset structure (a)] is 1.53 eV higher than that of the configuration N_s^a with the N atom in place of an O atom of pristine TiO_2. [Ti: light gray, O: dark gray (red), and N: gray (cyan) spheres.]

N_s^b, N_s^c, and N_s^d. Previous studies[11,12,17,18] have identified N_s^a as the most stable structure and our results agree with this finding. Compared to N_s^a, N_s^b, N_s^c, and N_s^d lie higher in energy (by 1.53, 0.9, and 3.6 eV) and they can be thought of as intermediate structures during migration of the dopant. In particular, N_s^a may first transform to N_s^b, followed by exchange of positions between N and its nearest O atom, and a final transformation to a neighboring N_s^a configuration. The rate-limiting step for this hopping event is the exchange transformation and the activation energy is 2.09 eV. Figure 5 depicts the intermediate configurations and energy variation in the rate-limiting segment of this hopping event. Another hopping path, with a higher E_a of 3.18 eV, involves transformation of N_s^a to N_s^c, exchange of N and O atoms, and change to a vicinal N_s^a structure.

As in previous studies,[12,18] the most stable N interstitial structures are the ones depicted in Fig. 6. N binds to an O atom of the network and can hop along the (100) and (010) directions through consecutive transformations between the structures N_i^a and N_i^b of Figs. 6(a) and 6(b). The activation energy for this transformation, which is also the diffusion barrier of a N interstitial in anatase TiO_2, is 1.23 eV. The energy variation and intermediate configurations during this hopping event are shown in Fig. 7. Another possibility is a transformation between the configurations N_i^a and N_i^c of Figs. 6(a) and 6(c). This hopping event allows change in the direction of diffusion and has an E_a of 1.66 eV.

Figure 8 shows the DOS of pristine anatase TiO_2 and anatase TiO_2 with substitutional and interstitial N impurities. For the N doping level, $n=1.39\%$ considered in this work, N_s^a induces defect states (denoted as DB1 in Fig. 8) that hybridize with the valence-band maximum (VBM) of TiO_2 narrowing the band gap by 0.1 eV. N_s^a also generates levels (DB2) in the gap about 0.8 eV above the VBM. N-related shallow acceptors and gap levels have been reported before, though older data for $n=1.56\%$, 6.25% and our results differ with respect to hybridization[12] with the VBM and the position of the gap level, respectively.[18] The extension of the valence band due to N-induced states is consistent with experimental data on the reduction in the energy threshold[6] for light absorption by N-doped TiO_2. In the case of N interstitials, the N_i^a structures create four defect levels within the TiO_2 band gap. These states are called DB3, DB4, DB5, and DB6 in Fig. 8. Previous studies have reported the creation of N interstitial-related levels in the gap, either[12] at 0.73 eV above VBM or a pair[18] of levels 0.85 and 1.6 eV higher than VBM.

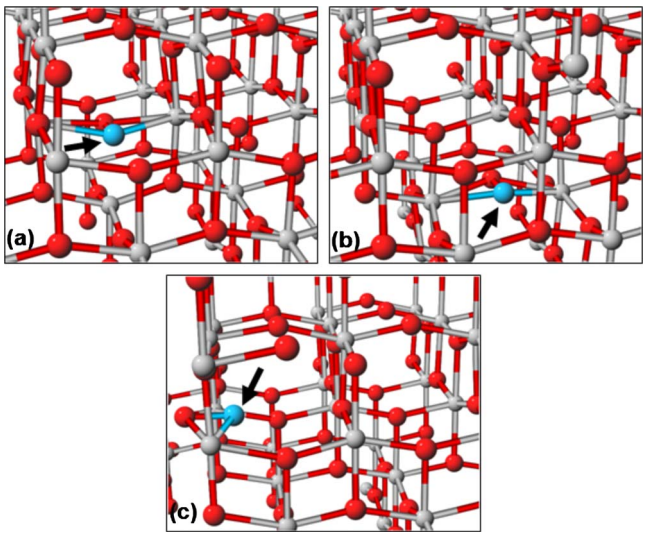

FIG. 6. (Color online) The most stable configurations of interstitial N impurities (shown with arrows) in anatase TiO_2. Hopping events from (a) to (b) and from (a) to (c) have activation energies of 1.23 eV and 1.66 eV, respectively. [Ti: light gray, O: dark gray (red), and N gray (cyan) spheres.]

C. Theoretical lattice constants and dopant stability

As mentioned above, the results presented thus far are based on the experimental lattice constants of anatase TiO_2. We now present results on the relative stability of the most important dopant structures using the lattice constants obtained by relaxation of the unit cell to the theoretical equilibrium configurations. The calculated a lattice constant is

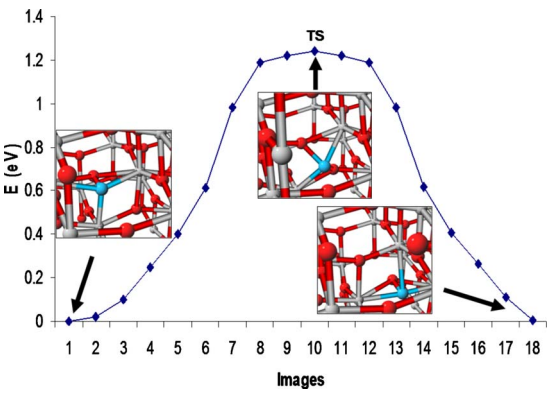

FIG. 7. (Color online) Energy variation and structures (insets) during diffusion of an interstitial N atom along the (100) direction of anatase TiO_2. TS is the transition state. [Ti: light gray, O: dark gray (red), and N gray (cyan) spheres.]

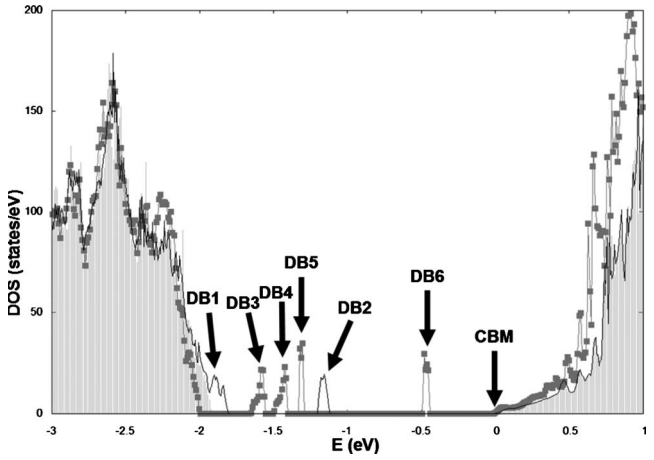

FIG. 8. Electronic DOS of pristine anatase TiO_2 (shaded) and TiO_2 with substitutional (solid line) and interstitial N (line with squares) impurities. Zero of energy is set at the CBM. The defect levels in the gap associated with substitutional (interstitial) N dopants are denoted DB1 and DB2 (DB3-DB6).

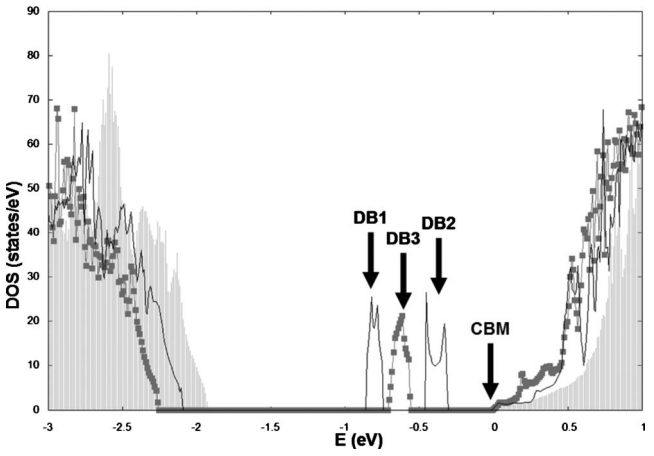

FIG. 9. Electronic DOS of pristine anatase TiO_2 (shaded) and TiO_2 with one substitutional (solid line) or interstitial C (line with squares) impurity in a supercell with 16 Ti atoms. Zero of energy is set at the CBM. DB1 and DB2 (DB3) denote the defect levels in the gap associated with substitutional (interstitial) C dopants.

equal to 3.819 Å, which is within 1% of the experimental value. A larger error with respect to experiment (overestimate by about 2%) is obtained for the c lattice constant of 9.709 Å. Similar, or larger, errors for the theoretical c constant have been obtained in previous DFT-GGA studies.[35]

Table II summarizes the energy differences and spin polarizations of the most stable dopant configurations when the calculations employ the theoretical lattice constants. There exist quantitative differences between the values of Table II and those of Table I, especially for the case of substitutional carbon dopants. Nevertheless, the order of the most important configurations in terms of relative stability is the same regardless of the choice of lattice constants (experimental or theoretical) made in the calculations.

D. Supercell size effects

The relative stability of C dopant configurations has also been checked with respect to the size of the supercell. Specifically, we used a larger $4\times4\times1$ supercell with 64 Ti and 128 atoms in the pristine case, and a smaller one ($2\times2\times1$) with 16 Ti and 32 O atoms. For the larger supercell, the nature of the most stable configurations is the same as those described above for the 108-atom cell. In particular, a structure similar to that of Fig. 1(c) has the lowest energy also for the 192-atom supercell while configurations that resemble those of Figs. 1(a), 1(b), 1(d), and 1(e) lie higher in energy by 1.10 eV, 0.35 eV, 0.88 eV, and 0.15 eV, respectively. Likewise, the 192-atom calculations show that the structure of Fig. 3(a) is more stable compared to that of Fig. 3(b) by 0.50 eV. In other words, for both substitutional and interstitial C dopants, the results based on the larger supercell agree with those of the 108-atom cell in terms of the nature of the most stable structures.

TABLE II. The relative energies and magnetic moments (M) of the most stable structures reported in Table I as obtained from calculations based on the theoretical lattice constants of anatase TiO_2.

Impurity type	Configuration	Energy (eV)	M (μ_B)
C_s	Fig. 1(b)	0.10	0.73
C_s	Fig. 1(c)	0.00	0.00
C_s	Fig. 1(d)	0.23	0.00
C_s	Fig. 1(e)	0.24	0.00
C_i	Fig. 3(a)	0.00	0.00
C_i	Fig. 3(b)	0.53	0.00
N_s	Fig. 1(a)	0.00	1.00
N_i	Fig. 6	0.00	1.00

The order of substitutional C dopant configurations with respect to relative stability is left unchanged when the smaller 48-atom supercell is employed. In this case, the calculations of total energies and densities of states were based on $5\times5\times5$ and $11\times11\times11$ k-point sampling, respectively. For this higher concentration of dopants, the structure of the type of Fig. 1(c) is more stable than those of Figs. 1(b) and 1(e) by 0.45 eV and 0.73 eV, respectively. In contrast, the order of relative stability is reversed for interstitial C impurities when the 48-atom cell is used. Specifically, the structure that resembles the configuration of Fig. 3(a) is less stable than that of Fig. 3(b) by 0.25 eV.

These results show that increasing the concentration of dopants can affect the stability of certain configurations and change the characteristics of equilibrium geometries. Moreover, differences in concentrations can result in variations in the electronic properties of doped TiO_2. For example, as shown in the densities of states plots of Fig. 9 and 10 for C and N impurities in the small 48-atom supercell, higher concentration affects both the value of the energy band gap of doped TiO_2 but also the number and position of gap states.

E. Interactions between dopants and point defects

In addition to transformations of dopant configurations, the evolution of impurities depends on interactions between

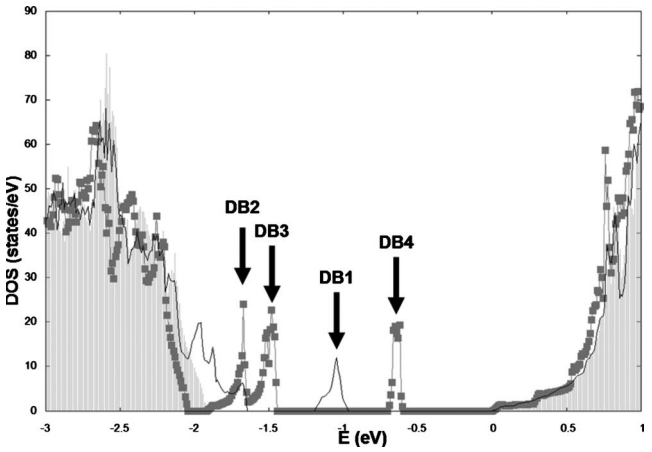

FIG. 10. Electronic DOS of pristine anatase TiO_2 (shaded) and TiO_2 with one substitutional (solid line) or interstitial N (line with squares) impurity in a supercell with 16 Ti atoms. Zero of energy is set at the CBM. The defect levels in the gap associated with substitutional (interstitial) N dopants are denoted DB1 (DB2, DB3, and DB4).

the extrinsic species and native point defects. For example, oxidation creates O interstitials that can interact with a substitutional N dopant to transform it to a N interstitial impurity. This process has been shown[12] to be exothermic by 0.8 eV, an energy gain that is confirmed by our calculations. We have found that the analogous oxidation step for C impurities in anatase TiO_2 is even more energetically favorable and releases 3.11 eV of energy. Other important interactions between impurities and native defects relate to the formation of complexes of vicinal substitutional dopants and O vacancies. The binding energy of a complex of substitutional C (N) and an O vacancy is 1.25 eV (2.26 eV). Finally, when an O vacancy arrives in the vicinity of a C (N) interstitial it can transform the latter to a substitutional dopant releasing 1.19 eV (3.43 eV) of energy.

The above notes on interactions between impurities and point defects make clear that the diffusivity of O vacancies and interstitials is a key factor for the dynamics of dopants in TiO_2. For this reason, we studied the kinetics of migration of native point defects in anatase TiO_2. An O vacancy can hop along $(10\bar{1})$ or $(01\bar{1})$ direction to the nearest O site with a very small barrier of only 0.25 eV. Repeated hopping steps of this type allows fast diffusion along the (100) or (010) direction. On the other hand, the hopping step that leads to change in the migration direction between (100) and (010) has a higher activation energy of 1.2 eV. A similar barrier is obtained for O interstitials, whose most stable configurations resemble the structures of Fig. 6 with the N impurity replaced by an O atom. Migration of the interstitial O atom along the (100) or (010) direction happens through processes similar to N_i^a to N_i^c transformations with an E_a of 1.18 eV. The activation energy for migration along the (001) direction is equal to 1.4 eV.

IV. DISCUSSION

Based on the stability and diffusivity of impurities and defects in TiO_2, several different scenarios that may lead to change in photocatalytic activity emerge. The diffusion barrier (1.18 eV) of O interstitial oxidation products suggests that heating at moderate temperatures in the range of 100–300 °C can activate their diffusion and ensuing transformations of substitutional dopants to interstitial impurities. As a result, the catalytic activity can be modified due to change in the position, or even elimination in the case of C, of levels in the gap.

The reverse interstitial to substitutional transformations can happen when interstitial impurities coexist, following doped-TiO_2 synthesis or implantation, with O vacancies. In this case, our results identify O vacancies as the very mobile species that can diffuse even at temperatures much lower than room temperature, find the impurities, and change them to substitutional dopants. Likewise, fast diffusing O vacancies can form complexes with dopants in anatase TiO_2. Change in the catalytic activity can also be observed following annealing at temperatures that can activate the migration of C and N impurities out of the bulk of anatase TiO_2. Based on the calculated barriers and the Arrhenius-type expression for the rate of processes we can estimate[29,30] that the diffusion of N interstitials becomes operative at about 100–300 °C while substitutional N and C impurities (substitutional or interstitial) start diffusing at higher, but not extremely high, temperatures. Finally, we should note that, in addition to the above processes, the stability and dynamics of dopants depends on charging effects. Preliminary results suggest that the relative stability of C dopant configurations may change in the presence of holes. A comprehensive study on the effect of charging of dopants will be presented elsewhere.

V. SUMMARY

In summary, we have identified lowest-energy configurations of C dopants in anatase TiO_2 structures that differ from predictions of previous studies. We have also provided estimates, based on calculations of the diffusion barriers of C and N dopants and native defects, of the temperatures required for migration of species, defect transformations, and defect complex formation. These processes can lead to significant changes in the photocatalytic activity of TiO_2 because of the accompanying modification of defects states in the anatase band gap.

ACKNOWLEDGMENT

The calculations used resources of the EGEE and HellasGrid infrastructure.

[1] A. Fujishima and K. Honda, Nature (London) **238**, 37 (1972).
[2] T. L. Thompson and J. T. Yates, Chem. Rev. **106**, 4428 (2006).
[3] P. V. Kamat, J. Phys. Chem. C **111**, 2834 (2007).
[4] T. Stergiopoulos, I. M. Arabatzis, G. Katsaros, and P. Falaras, Nano Lett. **2**, 1259 (2002).
[5] X. Chen and S. S. Mao, Chem. Rev. **107**, 2891 (2007).
[6] R. Asahi, T. Morikawa, T. Ohwaki, K. Aoki, and Y. Taga, Science **293**, 269 (2001).
[7] S. Sakthivel and H. Kisch, Angew. Chem., Int. Ed. **42**, 4908 (2003).
[8] S. U. M. Khan, M. Al-Shahry, and W. B. Ingler, Science **297**, 2243 (2002).
[9] A. B. Murphy, Sol. Energy Mater. Sol. Cells **91**, 1326 (2007).
[10] O. Diwald, T. L. Thompson, T. Zubkov, E. G. Goralski, S. D. Walck, and J. T. Yates, J. Phys. Chem. B **108**, 6004 (2004).
[11] C. Di Valentin, G. Pacchioni, and A. Selloni, Phys. Rev. B **70**, 085116 (2004).
[12] C. Di Valentin, G. Pacchioni, A. Selloni, S. Livraghi, and E. Giamello, J. Phys. Chem. B **109**, 11414 (2005).
[13] T. L. Thompson and J. T. Yates, Top. Catal. **35**, 197 (2005).
[14] N. Serpone, J. Phys. Chem. B **110**, 24287 (2006).
[15] M. Batzill, E. H. Morales, and U. Diebold, Phys. Rev. Lett. **96**, 026103 (2006).
[16] S. Livraghi, M. C. Paganini, E. Giamello, A. Selloni, C. Di Valentin, and G. Pacchioni, J. Am. Chem. Soc. **128**, 15666 (2006).
[17] K. Yang, Y. Dai, and B. Huang, J. Phys. Chem. C **111**, 12086 (2007).
[18] Z. Zhao and Q. Liu, J. Phys. D **41**, 025105 (2008).
[19] C. Di Valentin, G. Pacchioni, and A. Selloni, Chem. Mater. **17**, 6656 (2005).
[20] H. Kamisaka, T. Adachi, and K. Yamashita, J. Chem. Phys. **123**, 084704 (2005).
[21] H. Wang and J. P. Lewis, J. Phys.: Condens. Matter **18**, 421 (2006).
[22] G. Kresse and D. Joubert, Phys. Rev. B **59**, 1758 (1999).
[23] P. E. Blöchl, Phys. Rev. B **50**, 17953 (1994).
[24] J. P. Perdew and Y. Wang, Phys. Rev. B **45**, 13244 (1992).
[25] C. J. Howard, T. M. Sabine, and F. Dickson, Acta Crystallogr., Sect. B: Struct. Sci. **47**, 462 (1991).
[26] D. J. Chadi and M. L. Cohen, Phys. Rev. B **8**, 5747 (1973).
[27] O. Jepson and O. K. Andersen, Solid State Commun. **9**, 1763 (1971).
[28] G. Mills, H. Jónsson, and G. K. Schenter, Surf. Sci. **324**, 305 (1995).
[29] L. Tsetseris, N. Kalfagiannis, S. Logothetidis, and S. T. Pantelides, Phys. Rev. Lett. **99**, 125503 (2007); L. Tsetseris, S. Logothetidis, and S. T. Pantelides, Appl. Phys. Lett. **94**, 161903 (2009).
[30] L. Tsetseris and S. T. Pantelides, Acta Mater. **56**, 2864 (2008).
[31] L. Tsetseris, S. Wang, and S. T. Pantelides, Appl. Phys. Lett. **88**, 051916 (2006).
[32] L. Tsetseris and S. T. Pantelides, Phys. Rev. Lett. **97**, 116101 (2006).
[33] L. Tsetseris, G. Hadjisavvas, and S. T. Pantelides, Phys. Rev. B **76**, 045330 (2007).
[34] R. Asahi, Y. Taga, W. Mannstadt, and A. J. Freeman, Phys. Rev. B **61**, 7459 (2000).
[35] L. Thulin and J. Guerra, Phys. Rev. B **77**, 195112 (2008).